Optical properties of tungsten trioxide from first-principles calculations

Yuan Ping, Dario Rocca, and Giulia Galli

Phys. Rev. B **87**, 165203 — Published 16 April 2013

DOI: 10.1103/PhysRevB.87.165203

Optical Properties of Tungsten Trioxide from First Principles Calculations

Yuan Ping,[1,*] Dario Rocca,[1,2] and Giulia Galli[1,3]

[1] *Department of Chemistry, University of California, Davis, California 95616, USA*
[2] *Université de Lorraine, CRM², UMR 7036, Institut Jean Barriol, 54506 Vandoeuvre-lès-Nancy, France; CNRS, CRM², UMR 7036, 54506 Vandoeuvre-lès-Nancy, France*
[3] *Department of Physics, University of California, Davis, California 95616, USA*

Tungsten trioxide (WO_3) is an Earth abundant material of potential use as a light absorber for solar energy conversion processes. We carried out ab initio calculations of the band structure and absorption spectrum of WO_3 using many body perturbation theory and we present a detailed comparison of our results with photoemission and absorption data. We show that it is necessary to take into account multiple effects, including spin-orbit and electron-phonon interaction, and exciton binding, in order to correctly predict the measured optical gap. The absorption spectrum obtained by solving the Bethe Salpeter equation compares well with experiments over a wide energy range, and our calculations correctly account for the red shift observed experimentally upon N_2 intercalation in WO_3.

I. INTRODUCTION

Several transition metal oxides are promising materials for light absorption in photovoltaic and photoelectrochemical cells [1–5]. Hence the investigation of their opto-electronic properties is an active field of research. Titania (TiO_2) is the best studied light absorber oxide, since the pioneering experiments of Fujishima and Honda [6]. However its optical gap (3.0 eV [7]) is larger than desired to absorb visible light. Tungsten trioxide (WO_3) is another promising oxide for use in photo-electrochemical water-splitting systems [8–12]: it is stable against photocorrosion; its optical gap (2.6-2.7 eV) is smaller than that of TiO_2 and it may absorb sufficient visible light to generate modest photocurrents. Furthermore WO_3 electrochromism has additional applications, in e.g. building smart windows [13–15].

Surprisingly, despite many experimental studies devoted to WO_3, its opto-electronics properties are not well understood. Several measurements by UV-vis spectroscopy [16] and photoelectrolysis [17] yielded an indirect optical gap of 2.6 eV at room temperature(T), while Salje et al [18], who measured transmission spectra at room temperature, reported a direct gap of 2.58 eV. Similar to the case of TiO_2 [7, 19, 20], direct and inverse photoemission measurements of the fundamental gap of WO_3 led to a value much larger (0.6∼0.7 eV) [21, 22] than that of its optical gap, and this difference cannot be accounted for by the exciton binding energy. We note that optical and photoemission experiments were both conducted on the phase stable at room T. On the theoretical side, a coherent and consistent interpretation of experiments has not yet been formulated and the level of theory necessary to describe photoemission and absorption experiments of WO_3 is yet unclear. This lack of fundamental understanding of opto-electronic properties is common to several other oxides, and it has negatively impacted our ability to predict materials with desired properties for solar energy conversion.

In this paper we report ab initio calculations of the fundamental and optical gap of γ-WO_3, and of its absorption spectrum, carried out using many body perturbation theory(MBPT) [23, 24]. We carried out calculations of the band structure within the G_0W_0 approximation [25–27] and we solved the Bethe-Salpeter Equation (BSE) [23, 24] to obtain the optical spectra, using the method of Refs. [28, 29]. The electron phonon renormalization of the band gap was obtained by means of a Fröhlich Hamiltonian [30–32], where the high frequency and static dielectric functions and longitudinal optical phonon frequency were computed from first principles, using Density Functional Perturbation Theory (DFPT) [33]. Spin orbit interaction was included using fully relativistic pseudopotentials [34].

We show below that multiple effects need to be taken into account, in order to correctly predict the experimental optical gap, including spin-orbit and electron-phonon interaction, and exciton binding. Our computed quasiparticle gap including spin-orbit and electron-phonon interaction is smaller (∼0.4 eV) than that obtained from photoemission experiments, which most likely probed surface instead of bulk electronic gaps. Our computed absorption spectrum for simple cubic WO_3 agrees well with recent measurements on blue bronze [35], over a wide energy range. In addition to the pure oxide, we also considered di-nitrogen doping, which was shown[9, 10] to lower the band gap towards the visible range and thus to be beneficial for solar applications.

The rest of the paper is organized as follows: in Section II we describe our results for the photoemission gap and in Section III and IV we present calculations of the optical gap and spectra, respectively. Section V contains our conclusions.

* yping@ucdavis.edu

II. PHOTOEMISSION GAP

We first computed the electronic gap of WO_3 at several levels of theory and we compared our results with photoemission data (see Table I and Table II). We used the Quantum Espresso package [36] for all ground state calculations without spin orbit (SO) and the ABINIT code [37, 38] for those including SO; we used the Yambo code [25] for G_0W_0 calculations.

We considered both the room temperature monoclinic phase (γ-WO_3, see Fig. 1) and the simple cubic (SC) phase (unstable at atmospheric pressure but stable at 0.66 Gpa and 700℃ [39]). At room T, WO_3 has a perovskite structure that differs from that of the simple cubic lattice only by the location of the W atoms, that are off the octahedra centers; the tilt angles between octahedra deviate from 180°by 15°∼25°in the γ phase. As a result, the electronic structure of simple cubic and γ-WO_3 are similar: the top of the valence band consists of the O 2p states and the bottom of the conduction band is composed of W 5d states (slightly hybridized with O 2p states).

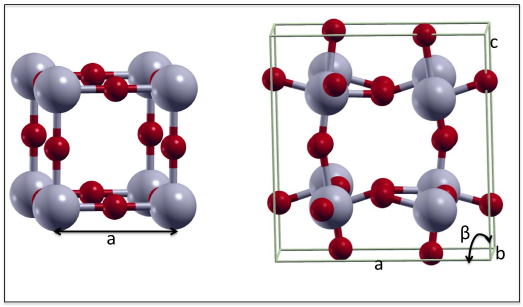

FIG. 1. The crystal structure of simple cubic WO_3(left) and γ-WO_3(right). WO_3 has the perovskite structure (ABO_3) where the central "A" site is not occupied.

All band gap calculations for γ-WO_3 were carried out at the experimental geometry, which is well established. At present there is a lack of consensus in optimized structures [10] using Density Functional Theory (DFT) with local density (LDA) [40, 41], PBE [42], or Van der Waals density functionals [43]. Calculations for SC were instead carried out at optimized geometries (Table I).

We used DFT/LDA, the modified ΔSCF method proposed in Ref 47, and MBPT within the G_0W_0 approximation. The computational details of the ΔSCF and G_0W_0 calculations are given in the Appendix A and B, respectively. The computed G_0W_0 band gap is converged within 0.1 eV with respect to all numerical parameters. In Table II we also report results of previous band gap calculations [46, 48, 49].

All DFT calculations with local or semi-local functionals greatly underestimate the measured gap, as expected, while the hybrid functional PBE0 [50] overestimates it.

TABLE I. Electronic band gap of simple cubic WO_3 computed at different levels of theory: LDA, ΔSCF and G_0W_0 and using the hybrid functional HSE06 [44, 45]. In this work all band gaps were computed at the LDA optimized geometry. In Ref 46, the geometry was optimized at the HSE06 level of theory.

	LDA	ΔSCF	HSE06	G_0W_0
Indirect($R \to \Gamma$)	0.55	1.57	1.54, 1.67[a]	1.78
Direct(Γ)	1.56	-	2.69	2.90

[a] From Ref 46

The HSE06 functional [44, 45] and the ΔSCF method yield very similar results for both γ-WO_3 and simple cubic WO_3, and they appear to moderately underestimate photoemission experiments; analogous findings were reported for rutile TiO_2, whose gap computed with the HSE06 functional, 3.05 eV [51], underestimates the measured photoemission gap (3.3-3.6 eV [19, 20]). The computed G_0W_0 band gap of γ-WO_3 is 3.26 eV, in apparent, excellent agreement with photoemission experiments (3.38±0.2 in Ref 21, and 3.28±0.14 in Ref 22).

TABLE II. Electronic band gap (eV) of γ-WO_3 computed using different levels of theory (acronyms are defined in the text). The first five rows of the table report results from the literature, while the remaining ones report results of this work. E_g^{opt} denotes the optical gap. The last column indicates whether the gap is direct (D), indirect (I) or pseudodirect (PD). In our calculations I and D gaps differ by less than ∼0.05 eV.

Theory	Band Gaps [eV]	Type
LDA	1.87[c],1.31 [48]	D,PD
PW91	0.90 [49],1.19 [46][b]	D
	1.36 [46][b],1.57 [46][b]	
RPBE	1.73 [52]	ID
B3LYP	3.13 [46]	D
HSE06	2.80 [46]	D
PBE0	3.94[c],3.67 [46]	D
ΔSCF	2.92[c]	-
G_0W_0	3.26[c]	D
G_0W_0(w/SO[a])	3.16[c]	D
G_0W_0(w/SO/e-ph[a])	2.86[c]-2.96[c]	D
Exp(UPS-IPES)	3.38±0.2 [21],3.28±0.14 [22]	-
E_g^{opt}	2.71[c]-2.81[c]	D
E_g^{opt}(exp) [17, 18, 53]	2.6-2.7(300K),2.8-2.9(0K)	ID,D

[a] SO: spin orbit; e-ph: electron phonon.
[b] Ref 46(**PW91**):1.19 eV computed by ultrasoft pseudopotentials; 1.36 eV computed by PAW pseudopotentials; 1.57 eV computed by Gaussian-type basis sets with a linear combination of atomic orbitals approach.
[c] In this work all band gaps were computed at the experimental geometry; the other calculations shown in the table were carried out at the optimized geometries of the corresponding functionals.

However additional, important effects need to be taken into account, before carrying out a meaningful comparison with experiment, e.g. spin-orbit (SO) effects and

corrections to the computed gap due to electron phonon interaction.

We discuss SO interaction first.The effect of spin orbit (SO) interaction on the band structure of solids containing W was so far examined only for bulk bcc W [54]. Large SO splittings up to 0.8 eV were found for some of the bands. In Table III, we compare the lattice constants and band gaps of simple cubic and γ-WO_3 (see Fig. 1) computed without and including SO coupling. In the former case we used non relativistic pseudopotentials (PP), while in the latter we used fully relativistic PP of the HGH form [34] which were generated from fully relativistic all electron calculations, i.e. by solving the two-component Dirac equation.

When including SO effects self-consistently in our LDA band structure calculations (see Fig. 2 and Fig. 3), we found a decrease of 0.1 eV in the band gap of γ-WO_3 obtained without SO (0.2 eV decrease in the case of simple cubic; see Table III). Such a reduction comes from the lowering of the conduction band minimum (CBM): the CBM states have mostly W 5d characters and are thus more affected than the O 2p states at the valence band maximum (VBM). We assumed that the magnitude of SO effects on the band gap is similar at the LDA and G_0W_0 level of theory (similar SO splittings, within 0.1 eV, were reported in LDA and GW calculations of several systems with heavy elements [55, 56]).

TABLE III. Equilibrium lattice parameters [lattice constants (Å), and angle (°), see Fig. 1] and direct (D) and indirect (I) band gaps (eV, fifth and sixth column) of simple cubic and γ-WO_3 computed with (w/SO) and without spin orbit interaction (wo/SO), using Density Functional Theory, and the local density approximation.

	Simple Cubic				
	a				
wo/SO	3.79				0.54(ID)1.62(D)
w/SO	3.79				0.34(ID)1.35(D)
	γ-WO_3				
	a	b	c	β	
wo/SO	7.35	7.45	7.66	90.6	1.30(D)(1.87(D)[a])
w/SO	7.38	7.45	7.66	90.4	1.20(D)(1.79(D)[a])

[a] Computed at the experimental geometry

Next we consider the effect of electron phonon (e-ph) interaction on the band gap of WO_3; such an effect was discussed in several papers for numerous semiconductors and insulators [57–62]. In general, including e-ph interaction decreases the value of the fundamental gap (E_g) even at zero temperature, due to zero point motion [57]. In principle, the e-ph renormalization of E_g may be obtained from ab initio calculations, as recently reported, e.g. for carbon diamond (8 valence electrons per unit cell) [58]. However these calculations are computationally very demanding, and they are still prohibitive for a system such as WO_3, with 256 electrons per unit cell. Therefore, following previous work on ionic crystals [63–65], we adopted a model Fröhlich Hamiltonian (FH)[30–32], assuming that the interaction of electrons with optical phonons is the dominant effect contributing to e-ph interaction. We note that the CBM of WO_3 is at Γ and thus the use of a FH is a reasonably accurate approximation. We also note that we did not consider small (Holstein) polaron formation (as, e.g. done in Refs. [66] and [67]) as these polarons do not affect the value of the optical gap, although they may affect photoluminescence.

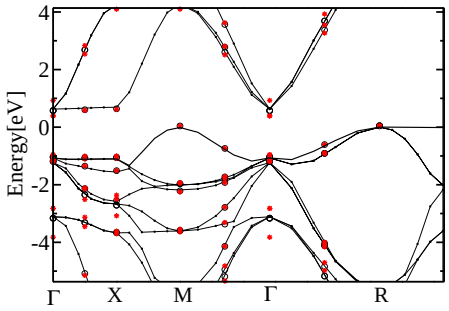

FIG. 2. Band structure of simple cubic WO_3 computed by including spin orbit (SO) interaction (black circles) and without SO (red stars).

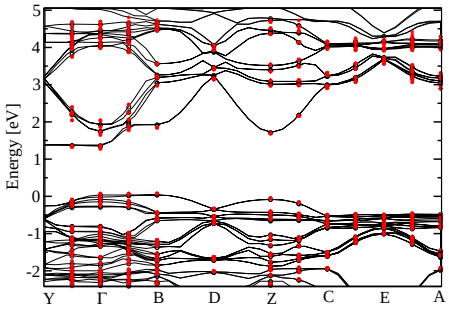

FIG. 3. Band structure of γ-WO_3 computed by including SO interaction (black circles) and without SO (red stars).

The renormalization of the lowest conduction band (ΔE) due to electron-optical phonon interaction can be evaluated by Rayleigh-Schrödinger(RS) perturbation theory and following Smondyrev [68] we have:

$$\Delta E = -\omega_{LO}[\alpha + 0.0159\alpha^2 + 0.000806\alpha^3 + O(\alpha^4)] \quad (1)$$

where ω_{LO} is the frequency of the longitudinal optical phonon, m_b is the conduction band effective mass, and α is a dimensionless coupling constant defined as:

$$\alpha = \frac{e^2}{\hbar}\left(\frac{m_b}{2\hbar\omega_{LO}}\right)^{1/2}\left(\frac{1}{\epsilon_\infty} - \frac{1}{\epsilon_0}\right). \quad (2)$$

Here ϵ_∞ and ϵ_0 are the high frequency and static dielectric constants, respectively, and a large difference between the two constants may be responsible for a large electron-phonon coupling.

We computed the optical phonon frequency and the dielectric constants of γ-WO_3 at different levels of the-

ory using DFPT [33], and we fixed the values of m_b to that reported by experiments by fitting Hall mobility values [69]. Our results are shown in Table IV: overall we found a downward shift of the CBM of 0.2-0.3 eV due to electron-phonon interaction. This value represents a lowerbound to the e-ph renormalization of the gap, since we did not include possible couplings of phonons with the valence band.

The coupling constant α computed at the LDA optimized geometry (1.74) is lower than the previously reported ones (approximately 3∼5) based on experimental data [70, 71]. The difference comes, at least in part, from the larger value of ϵ_∞ (6.53) obtained within LDA, compared to experimental data, varying between 3.2 and 6 [72, 73]. As pointed out in Ref 71, this variability probably stems from a great sensitivity of ϵ_∞ to small structural differences. Indeed we found that our results for ϵ_∞ are extremely sensitive to geometrical details. For example, the ϵ_∞ obtained as $\frac{1}{3}Tr(\varepsilon_\infty)$ (where ε_∞ is the macroscopic dielectric tensor) at the experimental geometry is 5.57, substantially smaller than the LDA optimized value of 6.53. The latter higher value originates from an underestimate of lattice distortions at the DFT/LDA level of theory, which in turn leads to a gap 0.5 eV lower than that computed at the experimental geometry. We note that using ω_{LO} = 70 meV[74] and ϵ_∞ computed at the experimental geometry, we obtained a coupling constant of 2.90, close to that reported by Refs. 70, 71. However, the use of ω_{LO} = 70 meV does not appear to have a robust justification. Interestingly, with the vdW-DF2 functional we obtained [10] results in better agreement with experiments for ϵ_∞ (5.63), ω_{LO} (125 meV) [71] and ϵ_0 (31) [75, 76].

When we included both SO and electron phonon interaction in the calculation of the γ-WO_3 quasiparticle gap we obtained a value of 2.9∼3.0 eV (see the value G_0W_0 (w/SO/e-ph) in Table II), which appears to underestimate the UPS-IPES gap measurements [21, 22]. We note that these measurements were performed using He I(21 eV) and He II(41 eV) sources and they have great surface sensitivity; hence the measured gap is most likely that of the surface, while we computed a bulk electronic gap. Higher photon energies (e.g. hard X-ray [77]) would be required to measure the bulk gap. Ref 22 noted that in a polycrystalline semiconductor a surface gap larger than that of the bulk is not unusual [78], due to possible structural and/or compositional differences between bulk and surface. Further studies are clearly necessary to clarify the difference between surface and bulk WO_3 quasiparticle gaps.

TABLE IV. Energy shift (ΔE) of the CBM due to electron-phonon interaction, obtained from Eq. 1. The effective mass of the lowest conduction band (1.75), was taken from Ref 69. All other parameters (the high frequency, ϵ_∞, and static, ϵ_0, dielectric constants and longitudinal phonon frequency ω_{LO}) were computed from first principles (see text).

ϵ_∞	ϵ_0	ω_{LO}(eV)	α	ΔE(eV)
6.53[a]	44.67[a]	0.134[b]	1.74	-0.241
6.53[a]	44.67[a]	0.070[c]	2.41	-0.176
5.57[d]	44.67[a]	0.134[b]	2.09	-0.291
5.57[d]	44.67[a]	0.070[c]	2.90	-0.214
5.63[e]	31.33[e]	0.125[e]	2.01	-0.260

[a] Optimized LDA geometry; averaged diagonal value.
[b] Optimized LDA geometry; highest optical phonon.
[c] From Ref 70
[d] Experimental geometry; averaged diagonal value.
[e] Optimized vdW-DF2 geometry.

III. OPTICAL GAP

We now turn to the discussion of the optical gap (E_g^{opt}) of WO_3, which was measured by UV-vis transmission spectroscopy and photoelectrolysis, yielding a well accepted experimental value of 2.6-2.7 eV [16–18] at room T. These measurements probed bulk properties. Data were analyzed using a Tauc plot(a power-law fitting of the absorption edge [79]): $\alpha h\nu = A(h\nu - E_g)^\beta$, with β =2 (1/2) for an indirect (direct) gap [80]; α is the absorption coefficient and A a constant. The direct or indirect nature of the fundamental optical gap of γ-WO_3 is still controversial. Several authors [16, 17] claimed the optical gap is indirect, because $\alpha(h\nu)$ is better fitted by a Tauc plot with $\beta = 2$; however, Saljie et al [18] fitted the absorption edge to a direct gap formula ($\beta = 1/2$) and obtained results (2.58 eV) similar to those with $\beta = 2$. We found (see Table B1 of appendix B) that the direct and indirect electronic gaps computed within G_0W_0 differ by less than 0.05 eV. We computed the optical gap of WO_3 by subtracting the exciton binding energy from the G_0W_0 gap, evaluated by including SO and e-ph interaction. The exciton binding (ϵ_b) was calculated as the difference between the first excitation energy of the optical spectrum (obtained by solving the BSE [28, 29]) and the G_0W_0 gap[81]. We found ϵ_b = 0.15 eV and a value of the optical gap of 2.7∼2.8 eV (see Table II), in accord with the value measured as a function of T with in the region of stability of γ-WO_3, extrapolated to 0 K, i.e. 2.8-2.9 eV[53].

IV. OPTICAL SPECTRA

Having found a good agreement between theory and experiment for the optical gap, we proceeded to analyze the optical spectrum of WO_3 first and then of N_2 doped WO_3. Most UV-vis spectra of WO_3 [82, 83] were measured over a narrow energy range nearby the fundamental absorption edge, and they are likely to be very sensitive to optical transitions with small intensity. Instead, measurements of reflectivity (e.g. with synchrotron radiation or by using ellipsometry) over a large energy range far from the absorption edge are less sensitive to the details of the edge, e.g. phonon-assisted transitions. Our spectra were

computed using the implementation of Refs [28, 29], at the BSE level of theory, and then did not include phonon assisted transitions and it is therefore meaningful to compare them with ellipsometry data. However, the latter are limited for pure single crystal γ-WO_3 [84], and rather uncertain. To the best of our knowledge, they were reported only in Ref 84, where it was noted that the ellipsometry measurements may have been influenced by contributions from domains with different crystallographic orientations. Therefore we choose to compare the spectrum of simple cubic WO_3 with that of sodium bronze ($Na_{0.65}WO_3$) (see Fig. 4), which has a band structure similar to that of simple cubic WO_3: the extra electrons from Na fill the conduction bands of the simple cubic lattice [85] without modifying its original band structure. We note that even though simple cubic WO_3 has a smaller band gap than that of the γ phase, since the energy of the Fermi level increases with increasing electron concentration from Na, and the Coulomb repulsion increases within the filled states, the onset of inter band transitions shift to higher energies as sodium is added to the system [84]. This results in a similar O2p-W5d gap in γ-WO_3 and in $Na_{0.65}WO_3$. Therefore, in order to compare with experiment, the computed BSE absorption spectrum of simple cubic WO_3 was shifted to the blue by the difference of the simple cubic WO_3 and γ-WO_3 band gaps, both obtained at the G_0W_0 level. The overall shape of the computed spectrum (Fig. 4) is in very good agreement with experiment

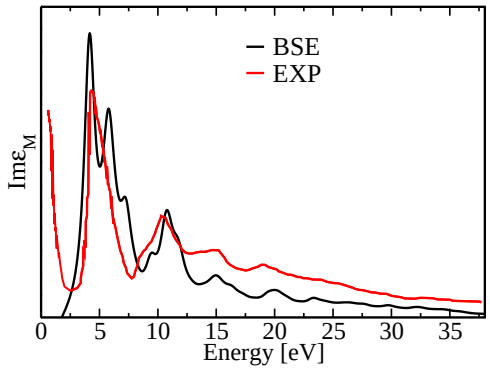

FIG. 4. Absorption spectrum (Imε_M) of WO_3 computed by solving the Bethe-Salpeter Equation (BSE) and that of $Na_{0.65}WO_3$ obtained by reflectivity experiments [35](EXP). A Lorentzian broadening of 0.04 Ry was added to the computed curve. The low energy rise of the experimental spectra is due to extra electrons from Na filling the bottom of the conduction band (see text).

To understand the influence of many body effects on the computed spectrum, we compared calculations at the BSE and Random Phase Approximation (RPA) level of theory (see Fig. 5). The RPA spectrum (including local field effects) using the LDA band gap presents two characteristic features: the band edge is red shifted due to the underestimate of the electronic gap by LDA, and the first peak has smaller intensity compared with the BSE spectrum, due to the lack of excitonic effects; as expected the RPA spectrum computed using the GW quasiparticle gap is shifted to higher energy, compared to that with the LDA gap. The BSE spectrum, which includes both quasiparticle corrections and excitonic effects is at lower energies, and the excitonic effects lead to an enhancement of the oscillator strength of the first peak, which compares well with experiment.

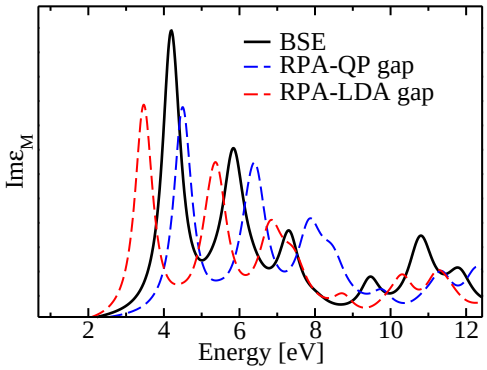

FIG. 5. Absorption spectrum (Imε_M) of WO_3 computed at different levels of theory: by solving the Bethe-Salpeter Equation (BSE); using the Random Phase Approximation (RPA) with quasiparticle (QP) G_0W_0 gap; and the RPA with LDA band gap. A Lorentzian broadening of 0.027 Ry was added to the computed curves.

As mentioned in the introduction, for solar applications it is desirable to lower the absorption gap of γ-WO_3 towards the visible range, and it was recently suggested that insertion of closed shell molecules in the oxide lattice may lead to a gap decrease. In particular, Refs. 9, 10 showed that γ-WO_3 intercalated with nitrogen molecules (N_2@WO_3) has a substantially smaller band gap than pure WO_3 (by about 0.8 eV), without exhibiting charged defects. Therefore we also examined the modifications of the absorption spectrum of the oxide upon insertion of N_2, although for computational convenience we considered a concentration higher than in experiments (We carried out calculations of N_2 in SC WO_3, with a di-nitrogen concentration of $1N_2$:$1WO_3$. The latter is higher than reported experimentally [9] and was chosen for computational convenience, and because we were interested in probing a qualitative effect of N_2 intercalation in WO_3). The computed GW-BSE spectrum of N_2@WO_3 in Fig. 6 shows two main features: the absorption edge is red shifted compared with that of pure WO_3, consistent with the experimental observation; the oscillator strength of the first two peaks is redistributed to higher energy. This indicates that the N_2 presence increases the screening of the electron hole interaction and hence it decreases the exciton binding between electron and hole pairs. Indeed, we found that the lowest exciton binding energy decreased by 0.05 eV upon N_2 intercalation. The redis-

tribution of the oscillator strength to higher energy is not desirable for solar applications; however, the presence of N_2 is mostly beneficial as the light absorption within the visible spectrum is enhanced by the presence of the molecule.

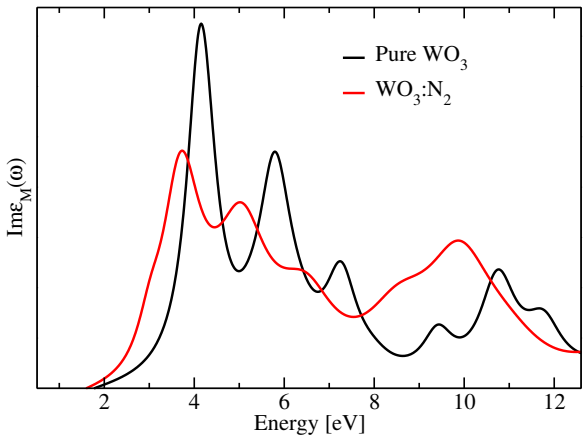

FIG. 6. Absorption spectrum of WO_3 and dinitrogen intercalated WO_3. A Lorentzian broadening of 0.027 Ry was added to the computed curves.

V. CONCLUSIONS

In summary, we showed that several effects need to be taken into account in order to correctly predict the optical gap of WO_3, including spin-orbit and electron-phonon interaction, and exciton binding. Many body perturbation theory at the BSE level, with fundamental gaps computed within the G_0W_0 approximation, yielded good agreement with measured spectra over a wide energy range, and correctly accounted for the red shift observed experimentally upon N_2 intercalation. We interpreted the difference between computed quasiparticle gaps and photoemission data (0.3-0.4 eV) as originating, at least in part, from the difference between measured surface gaps and computed bulk values. We also found minor differences ($\sim$0.05 eV) between indirect and direct minimum gap of WO_3, which may explain why different experiments [16–18] appeared to disagree on the character of the lowest gap of WO_3. We believe the detailed comparison between theory and experiments reported here for WO_3 will serve as a guide to carry out similar comparisons for other materials of interest for solar energy conversion.

This work was supported by grant NSF-CHE-0802907. We used the Extreme Science and Engineering Discovery Environment (XSEDE), which is supported by National Science Foundation grant number OCI-1053575. Computer time was also provided by NERSC. We thank Professor C. Fadley for useful discussions.

VI. APPENDICES

In appendix A and B, we report the computational details of ΔSCF and G_0W_0 calculations, respectively.

A. Computational details of ΔSCF calculations

We computed the band gap of WO_3 using the ΔSCF method proposed in Ref 47 as $E_g = [E(N_0+n)+E(N_0-n)-2E(N_0)]/n$, where N_0 is the number of valence electrons in the unit cell and $n = N_0/N^*$, where N^* is the number of electrons assumed to belong to the exchange and correlation (XC) hole; N^* was parametrized for hundreds of compounds in Ref 47. For our WO_3 calculations (LDA XC functional and spd valence electrons), $N^* = 63$. The band gap was computed at the room temperature experimental lattice constants. In the equation defining E_g, E is the total energy of the solid. The calculations were performed for charged periodic cells with neutralizing backgrounds. We note that the ΔSCF method of Ref 47 only yields the smallest band gap of the solid and it can not be used to compute the direct band gap for materials with indirect fundamental gaps. The results of ΔSCF calculations are reported in Table I and Table II for simple cubic and γ-WO_3, respectively.

B. Computational details of G_0W_0 calculations

In our G_0W_0 calculations we used the plasmon pole approximation(PPA) [86] to represent the frequency dependence of the dielectric matrix. PP models have proven to be relatively accurate for some energy bands of semiconductors and insulators, such as Si, Ge and LiCl [27]. However, Ref 62 found that the use of the Hybertsen-Louie PPA [27] leads to an overestimate of the gap of TiO_2 by 0.7-0.9 eV [62]. In addition, in Ref 87, the Hybertsen-Louie (HL) and von der LindenHorsch (vdLH) PP models were shown to strongly overestimate the band gap of ZnO compared with the full frequency integration, e.g. the contour-deformation (CD) approach [88]. Interestingly, the Godby-Needs (GN) [86] PP model gave results close to the CD approach for ZnO, and the convergence of GW calculations utilizing this model, with respect to the number of empty bands, was faster than that of the CD approach. Therefore we adopted the GN PP model and, for the case of the simple cubic structure, we compared the results with those of direct real frequency integration [89, 90] (RA, see Fig.B1), as implemented in the YAMBO package [25]. At the Γ point, the difference between G_0W_0 eigenvalues obtained with RA and the PPA (GN) was found to be less than 0.1 eV, while the difference between the direct band gap values is 0.14.

We also tested the convergence of the G_0W_0 direct band gap at Γ with respect to the number of bands included in the calculation (see Fig.B2), when using the

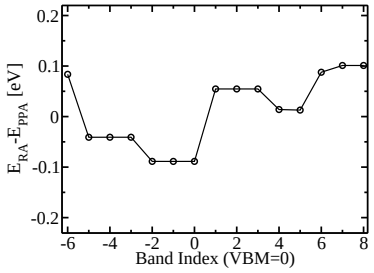

Fig. B1 . The difference between G_0W_0 eigenvalues at Γ for simple cubic WO_3, obtained using a plasmon pole approximation (E_{PPA}) and integration along the real axis (E_{RA}).

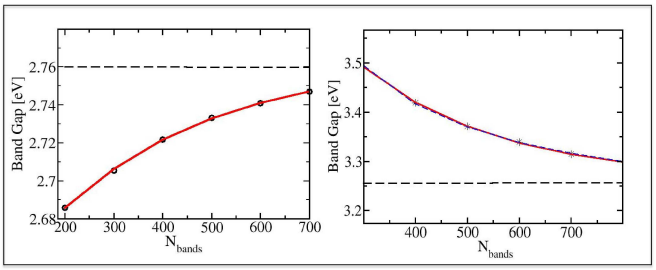

Fig. B2 . G_0W_0 direct band gap at Γ as a function of the number of bands (N_{bands}) included in the calculation, for simple cubic WO_3 (left panel) and γ-WO_3 (right panel). Spheres and stars represent the calculated G_0W_0 gaps using the PPA [86] for simple cubic and γ-WO_3, respectively. The results are fitted using two different functional forms described in the text, and displayed as red ($E(N) = E_0 - b.exp(-N/c)$) solid line and blue dotted line($E(N) = E_0 - b/N$).

GN model. For the simple cubic phase, the G_0W_0 direct gap extrapolated using the fitted function $E(N) = E_0 - b.exp(-N/c)$ is 2.76 eV (see Fig.B2 (left), where in the fit we used 6 points corresponding to the inclusion of 200 to 700 bands); the extrapolated value differs by only 0.05 eV from the one obtained with 300 bands. For the γ phase, the convergence was found to be slightly slower than for the simple cubic phase; we applied two different empirical fitting functions (see Fig.B2 right panel, where in the fit we used 6 points corresponding to the inclusion of 300 to 800 bands): $E(N) = E_0 - b/N$ and $E(N) = E_0 - b.exp(-N/c)$ which gave extrapolated values of 3.18 and 3.26 eV, respectively. The latter has a smaller root-mean-square relative error, therefore we retained this value as the best computed one. It differs by less than 0.05 eV from the band gap computed with 800 bands (3.30 eV). The numerical parameters entering our G_0W_0 calculations are: 37.5 Ry(16 Ry) for the size of the dielectric matrix and screened Coulomb potential of simple cubic (γ) WO_3, which yielded converged eigenvalues within 0.1 eV compared to 60 Ry energy cutoff for the dielectric matrix; we used 6x6x6 (3x3x3) kpts sampling for simple cubic (γ) WO_3 and 120 Ry for the ground state wavefunctions.

We also computed G_0W_0 eigenvalues for band edges at different k points (Table BI).

Table BI . Valence band maximum (VBM), conduction band minimum (CBM) and fundamental gap computed using DFT/LDA and G_0W_0 methods for γ-WO_3 at different k points.

	Γ	B	Z	D	Y	A	C	E
VBM								
LDA	0	-0.21	-0.024	-0.36	-0.14	-0.33	-0.48	-0.47
G_0W_0	0.29	0.025	0.26	-0.11	0.094	-0.12	-0.25	-0.24
CBM								
LDA	1.81	2.65	1.84	3.11	2.16	3.53	3.08	3.75
G_0W_0	3.59	4.49	3.62	4.98	3.98	5.42	4.93	5.67
Gap								
LDA	1.81	2.92	1.87	3.47	2.30	3.86	3.57	4.22
G_0W_0	3.30	4.46	3.36	5.09	3.88	5.54	5.18	5.91

The smallest LDA and G_0W_0 band gaps are direct at Γ(see Table BI), although the VBM and CBM at Z (0,0,1) are very close (within 0.05 eV) to respective eigenvalues at Γ (see Table BI). In fact, the lowest conduction state is between Γ to Z with a G_0W_0 eigenvalue of 3.58 eV, which indicates that the difference between direct and indirect gaps is negligible in γ-WO_3. As shown in Table BI, the G_0W_0 correction to the LDA gap is nearly the same at different k points, with variations less than 0.2 eV.

[1] M. G. Walter, E. L. Warren, J. R. McKone, S. W. Boettcher, Q. Mi, E. A. Santori, and N. S. Lewis, Chem. Rev. **110**, 6446 (2010).
[2] F. E. Osterloh, Chem. Mater. **20**, 35 (2008).
[3] S. Chen and L.-W. Wang, Chem. Mater. **24**, 3659 (2012).
[4] R. F. Berger and J. B. Neaton, Phys. Rev. B **86**, 165211 (2012).
[5] M. C. Toroker, D. K. Kanan, N. Alidoust, L. Y. Isseroff, P. Liao, and E. A. Carter, Phys. Chem. Chem. Phys. **13**, 16644 (2011).
[6] A. Fujishima and K. Honda, Nature **238**, 37 (1972).
[7] A. Amtout and R. Leonelli, Phys. Rev. B **51**, 6842 (1995).
[8] G. Hodes, D. Cahen, and J. Manassen, Nature **260**, 312 (1976).
[9] Q. Mi, Y. Ping, Y. Li, B. Cao, B. S. Brunschwig, P. G. Khalifah, G. A. Galli, H. B. Gray, and N. S. Lewis, J. Am. Chem. Soc. **134**, 18318 (2012).
[10] Y. Ping, Y. Li, F. Gygi, and G. Galli, Chem. Mater. **24**, 4252 (2012).
[11] J. A. Seabold and K.-S. Choi, Chemistry of Materials **23**, 1105 (2011).
[12] J. C. Hill and K.-S. Choi, The Journal of Physical Chemistry C **116**, 7612 (2012).
[13] S. K. Deb, Solar Energy Materials and Solar Cells **92**, 245 (2008).
[14] C. Granqvist, Solar Energy Materials and Solar Cells **60**, 201 (2000).
[15] C. Granqvist, Electrochimica Acta **44**, 3005 (1999).
[16] J. Kleperis, J. Zubkans, and A. R. Lusis, Proc. SPIE 2968 , 186 (1997).
[17] F. Koffyberg, K. Dwight, and A. Wold, Solid State Commun. **30**, 433 (1979).
[18] E. Salje, J. Appl. Crystallogr. **7**, 615 (1974).
[19] Y. Tezuka, S. Shin, T. Ishii, T. Ejima, S. Suzuki, and S. Sato, J. Phys. Soc. Jpn. **63**, 347 (1994).
[20] S. Rangan, S. Katalinic, R. Thorpe, R. A. Bartynski, J. Rochford, and E. Galoppini, J. Phys. Chem. C **114**, 1139 (2010).
[21] J. Meyer, M. Kroger, S. Hamwi, F. Gnam, T. Riedl, W. Kowalsky, and A. Kahn, Appl. Phys. Lett. **96**, 193302 (2010).
[22] L. Weinhardt, M. Blum, M. Bar, C. Heske, B. Cole, B. Marsen, and E. L. Miller, J. Phys. Chem. C **112**, 3078 (2008).
[23] G. Onida, L. Reining, and A. Rubio, Rev. Mod. Phys. **74**, 601 (2002).
[24] Y. Ping, D. Rocca, and G. Galli, Chem. Soc. Rev. **42**, 2437 (2013).
[25] A. Marini, C. Hogan, M. Grning, and D. Varsano, Comput. Phys. Commun. **180**, 1392 (2009).
[26] H.-V. Nguyen, T. A. Pham, D. Rocca, and G. Galli, Phys. Rev. B **85**, 081101 (2012).
[27] M. S. Hybertsen and S. G. Louie, Phys. Rev. B **34**, 5390 (1986).
[28] D. Rocca, D. Lu, and G. Galli, J. Chem. Phys. **133**, 164109 (2010).
[29] D. Rocca, Y. Ping, R. Gebauer, and G. Galli, Phys. Rev. B **85**, 045116 (2012).
[30] G. D. Mahan, *Many-Particle Physics* (Kuwer Academic, 2000) p. 433.
[31] M. P. Marder, *Condensed Matter Physics* (A Wiley-Interscience Publication, 2000) p. 618.
[32] C.G.Kuper and G.D.Whitfield, *Polarons and Excitons* (Plenum Press, 1962).
[33] S. Baroni, S. de Gironcoli, A. Dal Corso, and P. Giannozzi, Rev. Mod. Phys. **73**, 515 (2001).
[34] C. Hartwigsen, S. Goedecker, and J. Hutter, Phys. Rev. B **58**, 3641 (1998).
[35] D. Lynch, R. Rosei, J. Weaver, and C. Olson, J. Solid State Chem. **8**, 242 (1973).
[36] P. Giannozzi, S. Baroni, N. Bonini, M. Calandra, R. Car, C. Cavazzoni, D. Ceresoli, G. L. Chiarotti, M. Cococcioni, I. Dabo, A. Dal Corso, S. de Gironcoli, S. Fabris, G. Fratesi, R. Gebauer, U. Gerstmann, C. Gougoussis, A. Kokalj, M. Lazzeri, L. Martin-Samos, N. Marzari, F. Mauri, R. Mazzarello, S. Paolini, A. Pasquarello, L. Paulatto, C. Sbraccia, S. Scandolo, G. Sclauzero, A. P. Seitsonen, A. Smogunov, P. Umari, and R. M. Wentzcovitch, J. Phys.: Condens. Mat. **21**, 5502 (2009).
[37] X. Gonze, Z. Kristallogr. **220**, 558 (2005).
[38] X. Gonze, B. Amadon, P.-M. Anglade, J.-M. Beuken, F. Bottin, P. Boulanger, F. Bruneval, D. Caliste, R. Caracas, M. Cote, T. Deutsch, L. Genovese, P. Ghosez, M. Giantomassi, S. Goedecker, D. Hamann, P. Hermet, F. Jollet, G. Jomard, S. Leroux, M. Mancini, S. Mazevet, M. Oliveira, G. Onida, Y. Pouillon, T. Rangel, G.-M. Rignanese, D. Sangalli, R. Shaltaf, M. Torrent, M. Verstraete, G. Zerah, and J. Zwanziger, Comput. Phys. Commun **180**, 2582 (2009).
[39] W. A. Crichton, P. Bouvier, and A. Grzechnik, Mater. Res. Bull. **38**, 289 (2003).
[40] W. Kohn and L. J. Sham, Phys. Rev. **140**, A1133 (1965).
[41] N. D. Mermin, Phys. Rev. **137**, A1441 (1965).
[42] J. P. Perdew, K. Burke, and M. Ernzerhof, Phys. Rev. Lett. **77**, 3865 (1996).
[43] K. Lee, E. D. Murray, L. Kong, B. I. Lundqvist, and D. C. Langreth, Phys. Rev. B **82**, 081101 (2010).
[44] J. Paier, M. Marsman, K. Hummer, G. Kresse, I. C. Gerber, and J. G. Angyan, J. Chem. Phys. **124**, 154709 (2006).
[45] A. V. Krukau, O. A. Vydrov, A. F. Izmaylov, and G. E. Scuseria, J. Chem. Phys. **125**, 224106 (2006).
[46] F. Wang, C. Di Valentin, and G. Pacchioni, J. Phys. Chem. C **115**, 8345 (2011).
[47] M. K. Y. Chan and G. Ceder, Phys. Rev. Lett. **105**, 196403 (2010).
[48] M. N. Huda, Y. Yan, C.-Y. Moon, S.-H. Wei, and M. M. Al-Jassim, Phys. Rev. B **77**, 195102 (2008).
[49] G. A. d. Wijs, P. K. d. Boer, R. A. d. Groot, and G. Kresse, Phys. Rev. B **59**, 2684 (1999).
[50] J. P. Perdew, M. Ernzerhof, and K. Burke, J. Chem. Phys. **105**, 9982 (1996).
[51] A. Janotti, J. B. Varley, P. Rinke, N. Umezawa, G. Kresse, and C. G. Van de Walle, Phys. Rev. B **81**, 085212 (2010).
[52] R. Chatten, A. V. Chadwick, A. Rougier, and P. J. D. Lindan, J. Phys. Chem. B **109**, 3146 (2005).
[53] T. Iwai, J. Phys. Soc. Jpn. **15**, 1596 (1960).
[54] D. M. Bylander and L. Kleinman, Phys. Rev. B **29**, 1534 (1984).
[55] A. Svane, N. E. Christensen, M. Cardona, A. N. Chantis, M. van Schilfgaarde, and T. Kotani, Phys. Rev. B **81**,

245120 (2010).
[56] R. Sakuma, C. Friedrich, T. Miyake, S. Blügel, and F. Aryasetiawan, Phys. Rev. B **84**, 085144 (2011).
[57] M. Cardona, Solid State Commun. **133**, 3 (2005).
[58] F. Giustino, S. G. Louie, and M. L. Cohen, Phys. Rev. Lett. **105**, 265501 (2010).
[59] E. Cannuccia and A. Marini, Phys. Rev. Lett. **107**, 255501 (2011).
[60] M. Cardona and M. L. W. Thewalt, Rev. Mod. Phys. **77**, 1173 (2005).
[61] V. Perebeinos, J. Tersoff, and P. Avouris, Phys. Rev. Lett. **94**, 086802 (2005).
[62] W. Kang and M. S. Hybertsen, Phys. Rev. B **82**, 085203 (2010).
[63] B. C. Lee, K. W. Kim, M. Dutta, and M. A. Stroscio, Phys. Rev. B **56**, 997 (1997).
[64] M. E. Mora-Ramos, F. J. Rodrguez, and L. Quiroga, J. Phys.: Condens. Matter **11**, 8223 (1999).
[65] R. Riera, F. Comas, M. M. Ramos, and C. Trallero-Giner, Physica B **168**, 211 (1991).
[66] O. F. Schirmer and E. Salje, J. Phys. C **13**, L1067 (1980).
[67] O. Schirmer and E. Salje, Solid State Commun. **33**, 333 (1980).
[68] M. A. Smondyrev, Theor. Math. Phys. **68**, 653 (1986).
[69] J. M. Berak and M. Sienko, J. Solid State Chem. **2**, 109 (1970).
[70] A.-L. Larsson, B. E. Sernelius, and G. A. Niklasson, Solid State Ionics **165**, 35 (2003).
[71] G. A. Niklasson, L. Berggren, and A.-L. Larsson, Sol. Energy Mater. Sol. Cells **84**, 315 (2004).
[72] C. G. Granqvist, *Handbook of Inorganic Electrochromic Materials* (Elsevier, Amsterdam, 1995).
[73] M. J. DeVries, C. Trimble, T. E. Tiwald, D. W. Thompson, J. A. Woollam, and J. S. Hale, J. Vac. Sci. Technol., A **17**, 2906 (1999).
[74] Our computed ω_{LO} frequency (134 meV) at the fully optimized LDA geometry is in relatively good agreement with recent experiments by Gunnar [71], who reported longitudinal peaks at 50 and 123 meV. However Ref. 70 reported a single ω_{LO} value at 70 meV, which is close to the average, 75 meV, obtained using Gunnar's data: $\omega_{LO}^{-0.5} = \omega_{LO1}^{-0.5} + \omega_{LO2}^{-0.5}$. A much higher value (164 meV) was instead given in Ref. 91.
[75] I. Lefkowitz, M. Dowell, and M. Shields, J. Solid State Chem. **15**, 24 (1975).
[76] T. Hirose and K. Furukawa, Phys. Status. Solidi A **203**, 608 (2006).
[77] A. X. Gray, C. Papp, S. Ueda, B. Balk e, Y. Yamashita, Y. Yamashita, L. Plucinski, J. Minr, J. Braun, E. R. Ylvisaker, C. M. Schneider, W. E. Pickett, H. Ebert, K. Kobayashi, and C. S. Fadley, Nat Mater **10**, 759 (2011).
[78] M. Morkel, L. Weinhardt, B. Lohmuller, C. Heske, E. Umbach, W. Riedl, S. Zweigart, and F. Karg, Appl. Phys. Lett. **79**, 4482 (2001).
[79] D. L. Wood and J. Tauc, Phys. Rev. B **5**, 3144 (1972).
[80] P. Y. Yu and M. Cardona, *Fundamentals of Semiconductors: Physics and Material Properties* (Springer, New York, 1996).
[81] We note that a dense k point sampling is essential to obtain the well converged exciton binding energy. We used a 8x8x8 k point mesh.
[82] B. Cole, B. Marsen, E. Miller, Y. Yan, B. To, K. Jones, and M. Al-Jassim, J. Phys. Chem. C **112**, 5213 (2008).
[83] Z. Hussain, Appl. Opt. **41**, 6708 (2002).
[84] J. F. Owen, K. J. Teegarden, and H. R. Shanks, Phys. Rev. B **18**, 3827 (1978).
[85] F. Cora, M. G. Stachiotti, C. R. A. Catlow, and C. O. Rodriguez, J. Phys. Chem. B **101**, 3945 (1997).
[86] R. W. Godby and R. J. Needs, Phys. Rev. Lett. **62**, 1169 (1989).
[87] M. Stankovski, G. Antonius, D. Waroquiers, A. Miglio, H. Dixit, K. Sankaran, M. Giantomassi, X. Gonze, M. Côté, and G.-M. Rignanese, Phys. Rev. B **84**, 241201 (2011).
[88] M. Giantomassi, M. Stankovski, R. Shaltaf, M. Grning, F. Bruneval, P. Rinke, and G.-M. Rignanese, phys. status solidi (b) **248**, 275 (2011).
[89] A. Marini, R. Del Sole, A. Rubio, and G. Onida, Phys. Rev. B **66**, 161104 (2002).
[90] C. Rostgaard, K. W. Jacobsen, and K. S. Thygesen, Phys. Rev. B **81**, 085103 (2010).
[91] E. Iguchi and H. Miyagi, J. Phys. Chem. Solids **54**, 403 (1993).